Report 4282

ulation of a 4-Node
Element With
egrees of Freedom

ur

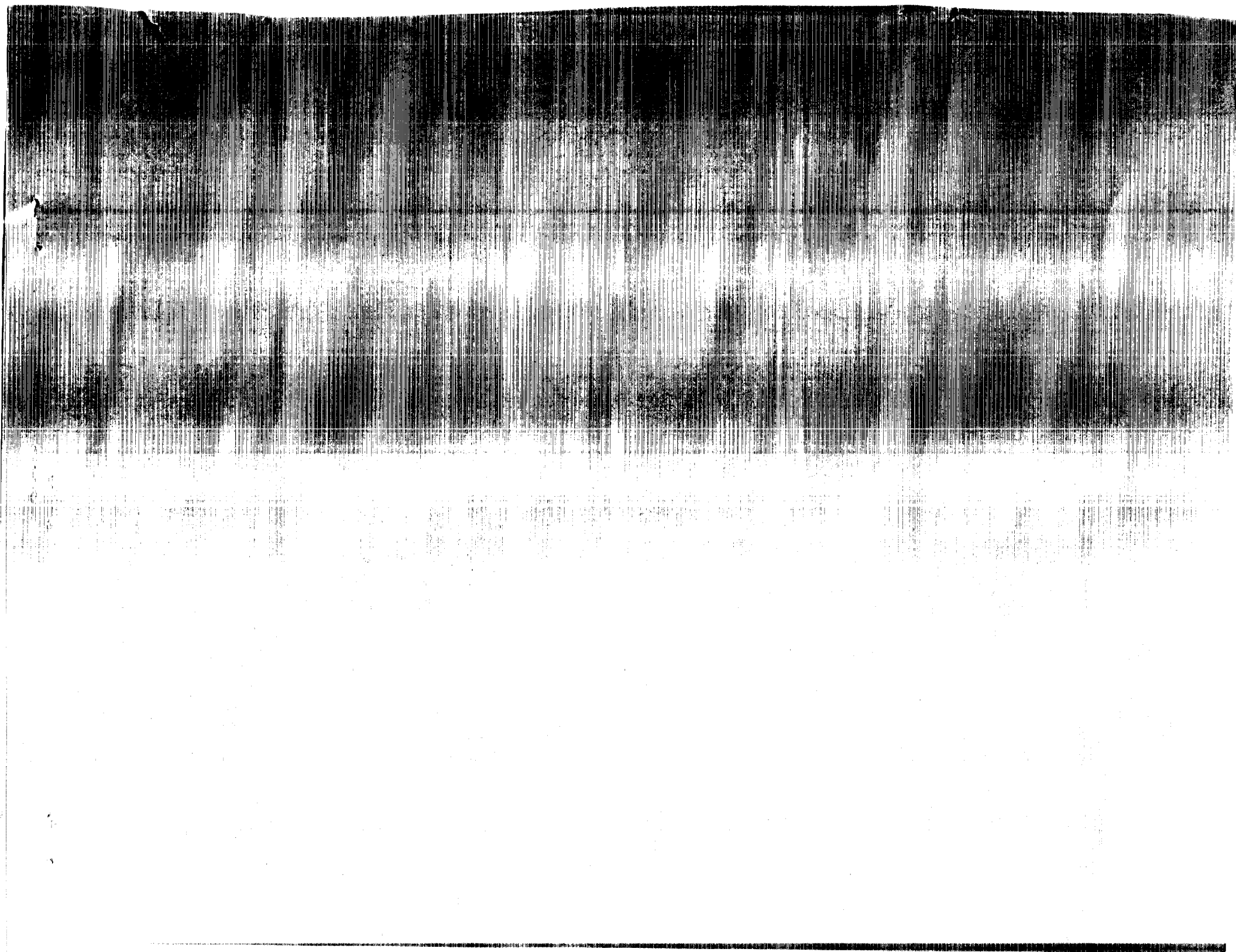

NASA Contractor Report 4282

Direct Formulation of a 4-Node Hybrid Shell Element With Rotational Degrees of Freedom

Mohammad A. Aminpour
Analytical Services & Materials, Inc.
Hampton, Virginia

Prepared for
Langley Research Center
under Contract NAS1-18599

National Aeronautics and
Space Administration
Office of Management
Scientific and Technical
Information Division

1990

Direct Formulation of a 4-Node Hybrid Shell Element with Rotational Degrees of Freedom

M. A. AMINPOUR
Analytical Services & Materials, Inc.
Hampton, VA 23666, U.S.A.

Abstract

A simple 4-node assumed-stress hybrid quadrilateral shell element with rotational or "drilling" degrees of freedom is formulated. The element formulation is based directly on a 4-node element. This direct formulation requires fewer computations than a similar element that is derived from an "internal" 8-node isoparametric element in which the midside degrees of freedom are eliminated in favor of rotational degrees of freedom at the corner nodes. The formulation is based on the principle of minimum complementary energy. The membrane part of the element has 12 degrees of freedom including rotational degrees of freedom. The bending part of the element also has 12 degrees of freedom. The bending part of the element uses the Reissner-Mindlin plate theory which takes into account the transverse shear effects. Quadratic variations for both in-plane and out-of-plane displacement fields and linear variations for both in-plane and out-of-plane rotation fields are assumed along the edges of the element. The element Cartesian-coordinate system is chosen such as to make the stress field invariant with respect to node numbering. The membrane part of the stress field is based on a 9-parameter equilibrating stress field, while the bending part is based on a 13-parameter equilibrating stress field. The element passes the patch test, is nearly insensitive to mesh distortion, does not "lock," possesses the desirable invariance properties, has no spurious modes, and produces accurate and reliable results.

Introduction

Finite element researchers face what seems to be an endless challenge to formulate simple 3-node and 4-node shell elements that are free from the usual deficiencies, such as locking, sensitivity to mesh distortion, non-invariance, and spurious modes. From the inception of the standard 4-node isoparametric element, researchers realized that this element exhibited severe locking and was very sensitive to mesh distortion. Ever since, researchers have considered a variety of methods to overcome these deficiencies. These methods have eliminated some of the shortcomings of the standard 4-node isoparametric element. However, some new difficulties such as non-invariance and spurious modes were introduced. Some of the milestones in the quest for a defect-free 4-node element are:

(1) Assumed-stress hybrid elements (Pian[1]).
(2) Reduced integration (Zienkiewicz et al.[2] and Pawsey and Clough[3]).
(3) Incompatible elements (Wilson et al.[4] and Taylor et al.[5]).

Another method of attacking the shortcomings of *membrane* elements is to include the nodal rotational or "drilling" degrees of freedom in the element formulation. In early attempts, these rotational degrees of freedom were used in cubic displacement functions. However, Irons and Ahmad demonstrated that this approach had serious deficiencies[6]. The elements formed in this manner force the shearing strain to be zero at the nodes, and these elements do not pass the patch test, which could produce erroneous results in some structural analysis problems. Recently researchers have used these rotational degrees of freedom in quadratic displacement functions with more success[7-11]. In previous papers, this latter method has been employed in the following way. First, the element is internally assumed to be an 8-node isoparametric element with 4 corner nodes and 4 midside nodes each having two displacement degrees of freedom, and the stiffness matrix associated with this "internal" element is calculated. Then, this stiffness matrix is condensed to that corresponding to a 4-node element with 12 degrees of freedom by associating the displacement degrees of freedom at the midside nodes with the displacement and rotational degrees of freedom at the corner nodes. MacNeal[9] has used this approach to develop a 4-node displacement-based *membrane* element with selective reduced-order integration. Yunus et al.[10] have also used this method to develop an assumed-stress hybrid/mixed *membrane* element. Aminpour[11] has also used this method to develop an assumed-stress hybrid/mixed *shell* element.

In this paper, a 4-node assumed-stress hybrid quadrilateral *shell* element with rotational degrees of freedom is presented. The formulation is based directly on a 4-node element from the beginning in contrast to elements whose formulations began with an "internal" 8-node element. Formulating the element in this manner bypasses the formation of the stiffness matrix for an 8-node isoparametric element and the subsequent transformation of this stiffness matrix to that corresponding to stiffness matrix of a 4-node element. This method is advantageous in that the element formulation is more direct and savings in computations are accrued. Results are presented for several standard test problems to establish the robustness of this element.

Hybrid Variational Principle

The classical assumed-stress hybrid formulation of Pian[1] is based on the principle of minimum complementary energy. The displacements are described on the element boundary and an equilibrating stress field is described over the the domain of the element. It was later recognized that the same method may be derived from the Hellinger-Reissner principle[12-14]. However, in the Hellinger-Reissner principle, the stress field does not have to satisfy the equilibrium equations a priori, and the displacement field has to be described over the domain of the element and not just on the boundaries. The stress field would then satisfy the equilibrium equations only in a variational sense. Therefore, the stress field may be described in the natural-coordinate system of the element which would make the element less sensitive to mesh distortion, and a proper selection of the stress field would make the element invariant with respect to node numbering. Because of these desirable properties, researchers have developed assumed-stress hybrid/mixed elements using the Hellinger-Reissner principle. For example, the membrane element in reference [10] and the

shell element in reference [11] were both developed using the Hellinger-Reissner principle. However, an assumed-stress hybrid 4-node shell element similar to that of reference [11] may also be easily formulated using the minimum complementary energy principle with the advantage being that only the displacements on the boundary of the element enter into the formulation. As such, the formulation is then based directly on a 4-node element rather than internally formulated as an 8-node element and then condensed to a 4-node element.

The invariant properties of the element is preserved by proper choice of a local element Cartesian-coordinate system. The local element Cartesian-coordinate system is shown in Figure 1 and is obtained by bisecting the angles formed by the diagonals of the element. The axes of this coordinate system are approximately parallel to the edges of the element for non-rectangular geometries (e.g., tapered and skewed elements) which would make the element less sensitive to mesh distortion. Upon node renumbering, this coordinate system is rotated by 90^0 increments. For example, if the connectivity for the element shown in Figure 1 is changed from 1-2-3-4 to 2-3-4-1, then the element local x-y axes in Figure 1 would rotate by 90^0. Therefore, selecting stress fields that are invariant with respect to a 90^0 rotation would make the element invariant with respect to node numbering.

The formulation of the element presented herein is based on the principle of minimum complementary energy. The details of the assumed-stress hybrid formulation using the minimum complementary energy principle have been extensively discussed in the literature, (e.g., see reference [1]), and hence, only a brief outline is given herein for completeness. The variational functional is given as

$$\Pi = -\frac{1}{2}\int_V \boldsymbol{\sigma}^T \mathbf{D}\boldsymbol{\sigma} dV + \int_S \boldsymbol{\sigma}^T \mathbf{n}\mathbf{u} dS - \int_{S_t} \mathbf{u}^T \mathbf{t_0} dS \tag{1}$$

where $\mathbf{D}$ is the compliance matrix of the material, $\boldsymbol{\sigma}$ is the stress array, $\mathbf{u}$ is the displacement array, $\mathbf{t_0}$ is the prescribed traction array, matrix $\mathbf{n}$ consists of the components of the outward unit normal to the boundary of the element such that $\mathbf{n}^T\boldsymbol{\sigma} = \mathbf{t}$ (traction array), V is the domain of the element, S is the boundary of the element, and S_t is the part of S where $\mathbf{t_0}$ is specified. The assumed-stress hybrid formulation is based on assuming an equilibrating stress field in the interior of the element as

$$\boldsymbol{\sigma} = \mathbf{P}\boldsymbol{\beta} \tag{2}$$

and assuming the displacement field only on the boundary of the element as

$$\mathbf{u} = \mathbf{N}\mathbf{q} \tag{3}$$

where the matrices $\mathbf{P}$ and $\mathbf{N}$ consist of the appropriate interpolating functions for stresses and displacements, respectively, and the coefficients $\boldsymbol{\beta}$ and $\mathbf{q}$ are the unknown stress parameters and nodal displacements and rotations, respectively.

The expressions for stresses in equation (2) and displacements in equation (3) are substituted into the functional Π of equation (1) and the variation of the functional with respect to the internal unknowns $\boldsymbol{\beta}$ is set to zero. This stationary condition gives

$$\boldsymbol{\beta} = \mathbf{H}^{-1}\mathbf{T}\mathbf{q} \tag{4}$$

where

$$\mathbf{H} = \int_V \mathbf{P}^T \mathbf{D} \mathbf{P} dV \tag{5}$$

$$\mathbf{T} = \int_S \mathbf{P}^T \mathbf{n} \mathbf{N} dS \tag{6}$$

Upon substitution of the expression for β in equation (4) into the functional Π of equation (1) and a subsequent variation of the functional with respect to the nodal unknowns $\mathbf{q}$ yields

$$\mathbf{K}\mathbf{q} = \mathbf{F} \tag{7}$$

where the stiffness matrix $\mathbf{K}$ is given by

$$\mathbf{K} = \mathbf{T}^T \mathbf{H}^{-1} \mathbf{T} \tag{8}$$

and the generalized force array $\mathbf{F}$ by

$$\mathbf{F} = \int_{S_t} \mathbf{N}^T \mathbf{t_0} dS \tag{9}$$

Formulation of 4-Node Quadrilateral Element

Displacement Field Description

As discussed previously, all three displacement components on the element boundary are assumed to vary quadratically and all three rotational components to vary linearly. The expressions for these boundary displacements and rotations were derived in detail in reference [11] and only the final results are given herein. The in-plane boundary displacements on edge 1 of Figure 1 are given by

$$\begin{aligned} u &= \frac{1}{2}(1-\xi)u_1 + \frac{1}{2}(1+\xi)u_2 + \frac{\Delta y_1}{8}(1-\xi^2)(\theta_{z2} - \theta_{z1}) \\ v &= \frac{1}{2}(1-\xi)v_1 + \frac{1}{2}(1+\xi)v_2 - \frac{\Delta x_1}{8}(1-\xi^2)(\theta_{z2} - \theta_{z1}) \end{aligned} \tag{10}$$

and the out-of-plane boundary displacement and rotations on edge 1 of Figure 1 are given by

$$w = \frac{1}{2}(1-\xi)w_1 + \frac{1}{2}(1+\xi)w_2 - \frac{\Delta y}{8}(1-\xi^2)(\theta_{x2} - \theta_{x1}) + \frac{\Delta x}{8}(1-\xi^2)(\theta_{y2} - \theta_{y1})$$

$$\begin{aligned} \theta_x &= \frac{1}{2}(1-\xi)\theta_{x1} + \frac{1}{2}(1+\xi)\theta_{x2} \\ \theta_y &= \frac{1}{2}(1-\xi)\theta_{y1} + \frac{1}{2}(1+\xi)\theta_{y2} \end{aligned} \tag{11}$$

where, Δx_1 and Δy_1 are the Δx and Δy of edge 1 with respect to the reference local element x-y coordinate system (e.g., $\Delta x_1 = x_2 - x_1$) and ξ is a non-dimensional coordinate

on edge 1 such that $\xi = -1$ at node 1 and $\xi = +1$ at node 2. It is worth mentioning here that the true nodal normal rotations are, of course, given by $\frac{1}{2}(\frac{\partial v}{\partial x} - \frac{\partial u}{\partial y})$ evaluated at the nodes. Hence, the terms θ_{zi} are not true nodal rotations, and they may be referred to as "rotational connectors"[7]. The description for the displacements and rotations on the other edges of the element are readily obtained.

The description for the in-plane rotation θ_z is similar to the out-of-plane rotations θ_x and θ_y. However, the description for the in-plane rotation θ_z is not shown here and it does not enter into the membrane formulation, while both out-of-plane rotations θ_x and θ_y enter into the bending formulation. Therefore, both membrane part and bending part of the element are formulated in the same manner. All three displacement components are quadratic functions, while all three rotations are linear functions. This conformity in the order of the approximating polynomials for all displacement components and all rotational components is very desirable in analysis of shell problems. The displacement and rotation descriptions in equations (10) and (11) allow for in-plane shearing strain and transverse shearing strains, respectively. This feature is in contrast to cubic interpolations of in-plane or out-of-plane displacements which force the in-plane shearing strain or the transverse shearing strains to be zero at the element nodes. As discussed previously, elements constructed using quadratic interpolation have been more successful. These elements pass the patch test which is a necessary condition for convergence to the correct solution. The elements using cubic interpolation, on the other hand, do not pass the patch test and perform poorly for some structural analysis problems[6].

Equations (10), when extended to all four sides of the element, indicate that for the membrane part of the element 4 in-plane rotational degrees of freedom in addition to the usual 8 in-plane displacement degrees of freedom are required to express the in-plane displacements as quadratic functions. The bending part of the element, on the other hand, is formulated in terms of the usual 12 out-of-plane displacement and rotational degrees of freedom and no additional degrees of freedom are required to express the out-of-plane displacement as a quadratic function.

Therefore, the membrane part of the element has 12 degrees of freedom. Two of these are the in-plane translational rigid body motions and one is the in-plane rotational rigid body motion. Of the nine remaining degrees of freedom, three represent the constant strain states, five represent higher-order strain states, and the final degree of freedom represents a special type of zero-energy or "spurious" mode. As discussed in reference [11], this zero-energy mode is of a special type and is different from other spurious mechanisms such as the hour-glass mode. This zero-energy mode is associated with a state of zero nodal displacements and equal nodal rotations Θ_z, which renders the in-plane displacements u and v in equation (10) to be zero on all edges of the element. This mode is shown in Figure 2 using a cubic interpolation for displacements and may be called the "zero displacement" mode[7]. As discussed in reference [11], this zero-energy mode appears because the displacements are based on the differences of the nodal rotations and not the nodal rotations themselves. Therefore, the membrane part of the element has, in fact, only 3 independent rotational degrees of freedom but is expressed in terms of 4 rotational degrees of freedoms. Hence, one of the rotational degrees of freedom is superfluous and

must be eliminated. This zero-energy mode may be eliminated simply by prescribing at least one rotational degree of freedom in the entire finite element model of the structure.

As discussed earlier, the bending part of the element also has 12 degrees of freedom. One of these is the out-of-plane translational rigid body motion and two of these are the out-of-plane rotational rigid body motions. Of the nine remaining degrees of freedom, three represent the constant curvature states, two represent the constant transverse shear strain states, and the other four represent higher-order strain states. No zero-energy modes are associated with the bending part of the element despite the fact the out-of-plane displacement is also expressed in terms of the differences of nodal rotations. The reason is that the out-of-plane rotations θ_x and θ_y enter into the bending formulation to account for each one of the out-of-plane nodal rotations, but the in-plane rotation θ_z does not enter into the membrane formulation.

Stress Field Description

The stress field should be selected in such a manner that no spurious zero-energy mode is produced. A spurious zero-energy mode is produced when the product of a selected stress term and the strains that are derived from the displacement functions produces zero strain energy under a particular, but not trivial, deformational displacement field. In order to avoid spurious zero-energy modes, each independent stress term must suppress one independent deformation mode. Therefore, the minimum number of stress terms required is equal to the number of degrees of freedom of the element less the number of rigid body modes. Spurious zero-energy modes generally occur for regular geometries such as rectangular planar elements and brick solid elements and disappear for irregular geometries[15]. As discussed previously, the stress fields (membrane and bending) are expressed in a proper Cartesian-coordinate system and selected in such manner as to remain invariant upon node renumbering. This coordinate system is shown in Figure 1 and the stress fields that are expressed in this coordinate system must remain invariant under a 90^0 rotation to remain invariant under node renumbering. The selected stress fields must also satisfy the equilibrium equations in order to be used in the functional Π of equation (1).

As discussed previously, the membrane part of the element has 12 degrees of freedom, three of which are due to the in-plane rigid body motions. Therefore, a stress field with a minimum of 9 independent parameters is needed to describe the membrane stress (resultant) field. The following equilibrating stress (resultant) field is considered for the membrane part

$$\begin{aligned} N_x &= \beta_1 + \beta_4 y + \beta_6 x + \beta_8 y^2 \\ N_y &= \beta_2 + \beta_5 x + \beta_7 y + \beta_9 x^2 \\ N_{xy} &= \beta_3 - \beta_6 y - \beta_7 x \end{aligned} \tag{12}$$

This stress (resultant) field is expressed in the local element Cartesian-coordinate system shown in Figure 1 and is similar to that proposed by reference [11]. However, in reference [11] the Hellinger-Reissner principle was used, and the stresses were expressed in the natural-coordinate system. The first five terms of the stress field in equation (12) represent the stress field that was used in the original 4-node (see reference [1]) assumed-stress hybrid

membrane element with 8 degrees of freedom which did not include any normal rotational degrees of freedom. The remaining four terms are present to suppress the four rotational degrees of freedom present in this formulation. As discussed in reference [11], this selection of stress field produces no spurious zero-energy modes for the assumed in-plane displacement field described in equation (10).

As discussed earlier, the bending part of the element has 12 degrees of freedom, three of which are due to the out-of-plane rigid body motions. Therefore, a stress field with a minimum of 9 independent parameters is needed to describe the bending stress field. The following equilibrating stress (resultant) field is selected here for the bending part

$$\begin{aligned} M_x &= \bar{\beta}_1 + \bar{\beta}_4 y + \bar{\beta}_6 x + \bar{\beta}_8 xy \\ M_y &= \bar{\beta}_2 + \bar{\beta}_5 x + \bar{\beta}_7 y + \bar{\beta}_9 xy \\ M_{xy} &= \bar{\beta}_3 + \bar{\beta}_{10} x + \bar{\beta}_{11} y + \frac{1}{2}\bar{\beta}_{12} x^2 + \frac{1}{2}\bar{\beta}_{13} y^2 \end{aligned} \tag{13}$$

The transverse shearing forces Q_x and Q_y are obtained using the equilibrium equations

$$\begin{aligned} Q_x &= \frac{\partial M_x}{\partial x} + \frac{\partial M_{xy}}{\partial y} \\ Q_y &= \frac{\partial M_{xy}}{\partial x} + \frac{\partial M_y}{\partial y} \end{aligned} \tag{14}$$

which gives

$$\begin{aligned} Q_x &= (\bar{\beta}_6 + \bar{\beta}_{11}) + (\bar{\beta}_8 + \bar{\beta}_{13}) y \\ Q_y &= (\bar{\beta}_7 + \bar{\beta}_{10}) + (\bar{\beta}_9 + \bar{\beta}_{12}) x \end{aligned} \tag{15}$$

This stress (resultant) field is expressed in the local element Cartesian-coordinate system shown in Figure 1 and is similar to that of reference [11]. However, in reference [11], the Hellinger-Reissner principle was used and the stresses were expressed in the natural-coordinate system. The stress (resultant) field given by equations (13) and (15) is obtained by integrating, through the thickness, the stress field that was derived in references [16-18]. The stress field in references [16-18] was derived by expressing the stress components as power series in the plate thickness, substituting these stresses into the continuum equations of elasticity, and equating the coefficients of like powers of the plate thickness. This 13 parameter selection of stresses for the bending part is less sensitive to geometric distortion than a 9 parameter selection obtained from a degenerate solid model[19]. This selection of stresses produces no spurious zero-energy modes. It is observed that both the membrane and bending stress (resultant) fields remain invariant upon node renumbering.

In this paper, the Reissner-Mindlin plate theory is used for the bending part. The bending part of the element is of class C^0 and takes into account the effects of transverse shear deformations by assuming constant transverse shear strains through the thickness of the plate. This assumption means that the transverse shear stresses are also constant through the thickness of the plate. However, generally the transverse shear stresses are zero on the plate surfaces. Therefore, a parabolic variation of transverse shear stresses and strains through the plate thickness is more reasonable. To account for this discrepancy, a static correction factor of 5/6 is included in the transverse shear strain energy, see Reissner[20].

Other Element Matrices

Formulating the element in the manner described above, provides a direct derivation of the linear stiffness matrix for a 4-node assumed-stress hybrid shell element. However, this methodology is not carried over to other element matrices because, for element matrices such as mass and geometric stiffness matrices the displacement functions over the domain of the element are required. The derivation of these element matrices are based on the "internal" 8-node element described in reference [11].

The surface traction and pressure loads are assumed to vary bilinearly over the element surface and the force vector **F** is calculated for the "internal" 8-node element. This force vector is then condensed to that of the 4-node element using the approximations for the midside degrees of freedom described in reference [11]. The calculation of the force vector **F** for line loads, however, are conducted based directly on the 4-node element by assuming linear variation of line loads along the edges of the element and using the displacement and rotation shape functions of equations (10) and (11).

Numerical Results

The performance of the 4-node quadrilateral shell element developed in this paper is evaluated in this section. The element has been implemented in the NASA Langley CSM Testbed software system[21] using the generic element processor template[22]. Selected test problems are reported including the patch test, the straight cantilever beam, the curved cantilever beam, Cook's tapered and swept panel, the Scordelis-Lo roof, and Morley's spherical shell problem. The assumed-stress hybrid 4-node quadrilateral shell element derived in this paper will be referred to as AQD4 (Assumed-stress Quadrilateral Direct 4-node element) in the following discussion for convenience. The results for the present element are compared with the results using the QUAD4 element of the MSC/NASTRAN from reference [23], the Q4S element from reference [9], the AQ element from reference [10], the ES1/EX47, ES5/E410, and ES4/EX43 elements of the NASA Langley CSM Testbed, and the AQR8 element of reference [11]. A brief description of these elements is presented in the appendix for completeness. The dimensions and properties for the test problems are chosen in consistent units.

Patch Test

As the first test of the accuracy of the element, the patch test problem suggested in reference [23] is solved. The patch is shown is Figure 3. Elements are of arbitrary shape patched together to form a rectangular exterior boundary. As such, boundary conditions corresponding to constant membrane strains and constant bending curvatures are easy to apply. The applied displacement boundary conditions and the theoretical solutions are also shown in Figure 3. The ability of the element to reproduce constant states of strains is an essential requirement for achieving convergence to the correct solution as the finite element mesh is refined. This requirement is observed by considering an individual element within a mesh with a complicated stress field. As the mesh is refined, the stresses within the elements tend towards a uniform value. Therefore, elements that cannot produce a state of constant strains should not be trusted to converge to the correct solution as the mesh is

refined[6]. The present element (AQD4) passes both the membrane and the bending patch tests with no error. The recovered strains and stresses are both exact.

Straight Cantilever Beam

As a second test, the straight cantilever beam problem suggested in reference [23] is solved for the three discretizations (six elements) shown in Figure 4. The constant and linearly varying strains and curvatures are produced by applying loads at the free end of the beam to test the ability of the element to recover these states of deformations. The theoretical results for extension, in-plane shear, out-of-plane shear, and in-plane moment are simply calculated from the elementary beam theory including shear deformations. The theoretical result for the twist is .03406, according to Timoshenko and Goodier's Theory of Elasticity[24]. Reference [23] quotes the answer to be .03208. Analysis with three successively refined meshes converged to .03385 which is much closer to the the theory of elasticity solution than to that of reference [23]. Therefore, the solution from the theory of elasticity is taken herein for normalization purposes. Normalized results for the present element along with the results for other elements are shown in Table 1. These results indicate that all elements perform well for the rectangular mesh. However, for the trapezoidal and parallelogram meshes which contain considerable amount of distortion, only the Q4S, the AQR8, and the present element (AQD4) perform well. It is noted that the results (except for the twist end load) are only slightly affected due to the fact that in this paper the stress field is expressed in the Cartesian-coordinate system. This means that for higher-order displacement functions it becomes less important to describe the stresses in the natural-coordinate system. The present element produces an error of less than 3.5% for all meshes and loads which indicates the insensitivity of the present element to mesh distortion. The present element also gives very good results for the parallelogram mesh with a twist end load, while the AQR8 produces an error of 15.9%.

Curved Cantilever Beam

Next, the curved cantilever beam problem shown in Figure 5 is solved. The beam is formed by a 90^0 circular arc. In-plane or out-of-plane loads are applied at the free end to produce in-plane and out-of-plane states of deformations, respectively. The theoretical solutions are taken to be those quoted in reference [23]. The normalized results from the present element are tabulated in Table 2. Results using other elements are also shown in Table 2 for comparison. For this problem, the mesh is distorted only slightly and the results for all elements are good. However, the AQR8 and the present element (AQD4) perform better than the other elements. Once again, it is noted that the results are only slightly affected due to the fact that in this paper the stress field is expressed in the Cartesian-coordinate system.

Cook's Tapered and Swept Panel

The tapered and swept panel with one edge clamped and the other edge loaded by a distributed shear force is analyzed next (see Fig. 6). This problem was used by Cook and many other researchers to test the sensitivities of finite elements due to geometric distortions. The panel was analyzed by a coarse 2×2 mesh and a finer 4×4 mesh. The reference solution for the vertical displacement at point C is taken to be 23.90 as quoted in reference [10]. The normalized results for the present element along with the results for

other elements are shown in Table 3. In this problem, the mesh is distorted only slightly and all elements produce reasonable results. The AQR8 and the present element (AQD4) however, produce results that are closest to the reference solution.

Scordelis-Lo Roof

The Scordelis-Lo roof is shown in Figure 7. This structure is a singly-curved shell problem in which both the membrane and bending contributions to the deformation are significant. The result reported in most papers is the vertical displacement at the midpoint of the free-edge. The theoretical value for this displacement is quoted in reference [25] to be 0.3086, but the normalization value quoted in reference [23] is 0.3024. The latter value is also used herein for normalization purposes. Because of symmetry, only one quadrant of the problem is modeled. The mesh on one quadrant is chosen to be N×N for N=2,4,6,8,10 (N=number of elements along each edge) to show the convergence of the solutions for the present element. The results of the normalized displacement at the midside of the free-edge are shown in Table 4. For this problem, the mesh is made of uniform rectangular-shaped elements and all the elements in the table perform well. It is observed that convergence rate to the reference solution for the present element is roughly the same as the other elements and the addition of the rotational degrees of freedom does not affect the convergence rate of the present element for this problem.

Morley's Spherical Shell

As a final test of the present element, the pinched hemispherical shell problem shown in Figure 8 is analyzed. The equator of the shell is chosen to be a free edge so that the problem represents a hemisphere loaded at four points. The load is alternating in sign at 90^0 intervals, and an 18^0 hole is present at the top of the hemisphere to avoid needing to model a pole. This structure is a doubly-curved shell problem and both membrane and bending contributions to the deformation state are significant. Because of symmetry, only one quadrant of the problem is modeled. The mesh on one quadrant is chosen to be N×N for N=2,4,6,8,10,12 (N=number of elements along each edge) to show the convergence of the solutions for the present element. The results of the normalized displacements at the load points are shown in Table 5. The theoretical displacement for normalization purposes is taken to be .0940 from reference [23]. It is seen that the AQR8 and the present element (AQD4) converge to the correct solution more slowly. In fact, a 14×14 mesh produced a normalized result of .952 and a 16×16 mesh produced a normalized result of .972 for both AQR8 and AQD4. The slower convergence of these elements for this problem is attributed to the fact that nearly all of the strain energy is bending energy even though the membrane stiffness is much larger than the bending stiffness. Consequently, any small amount of membrane-bending coupling strongly affects the stiffness of the shell. This membrane-bending coupling comes about by the coupling between the normal or "drilling" rotation and the bending rotations by the changes in slope at element intersections[9]. The incorrect geometry representation causes the slow convergence for these elements. This behavior shows both the importance and the need for more accurate geometry representations of shell problems. In reference [9], MacNeal also concluded that the Q4S element converges slower than the QUAD4 element for this problem for the reasons discussed. However, the Q4S does converge faster than the AQR8 and AQD4 elements for this problem.

Conclusions

A simple 4-node quadrilateral shell element with 24 degrees of freedom has been developed which alleviates most of the deficiencies associated with such elements. The element is based on the assumed-stress hybrid formulation and uses the principle of minimum complementary energy. The membrane part of the element has 12 degrees of freedom and includes the drilling (in-plane rotational) degrees of freedom at the nodes. The bending part of the element also has 12 degrees of freedom. The bending part is of class C^0 and takes into account the effects of transverse shear deformations. Both in-plane and out-of plane displacements are assumed to have quadratic variations along the edges of the element, while both in-plane and out-of-plane rotations are assumed to vary linearly. A 9-parameter stress field is assumed for the membrane part and a 13-parameter stress field is assumed for the bending part. The assumed stress fields satisfy the equilibrium equations. The formulation of the element is simple and straightforward. The element formulation is derived directly for a 4-node element. This approach is in contrast to 4-node elements with rotational degrees of freedom which are derived from "internal" 8-node isoparametric elements by eliminating the midside degrees of freedom in favor of rotational degrees of freedom at the corner nodes. This method therefore, bypasses the formation of the stiffness matrix for an 8-node element and the subsequent transformation of this stiffness matrix to that of a 4-node element, resulting in savings of computer time. Although, the stiffness matrix derivation is based directly on a 4-node element, most of the other element matrices such as the mass matrix still are derived based on an "internal" 8-node element which makes the derivation and implementation of the element somewhat awkward.

The element has been demonstrated to be accurate, pass both membrane and bending patch tests, is nearly insensitive to mesh distortion, does not "lock", and has no spurious modes. The element also has the desirable property of being invariant with respect to node numbering. The fact that the stresses are expressed in a Cartesian-coordinate system affects the results only slightly for the moderately distorted elements in the test problems considered. This behavior indicates that it becomes less important to describe the stresses in the natural coordinate system when higher-order displacement functions are present. Additional savings are accrued in this method by expressing the stresses in a Cartesian-coordinate system because, the tensor transformations of tensorial stresses in the natural-coordinate system to physical stresses are not performed.

The results obtained herein are very encouraging and warrant further research to make the derivation of all element matrices more direct and to extend the formulation to stability analysis, dynamic analysis, and nonlinear analysis.

References

1. Pian, T. H. H.: Derivation of Element Stiffness Matrices by Assumed Stress Distributions. AIAA Journal, Vol. 2, 1964, pp. 1333-1336.

2. Zienkiewicz, O. C.; Taylor, R. L.; and Too, J. M.: Reduced Integration Techniques in General Analysis of Plates and Shells. International Journal for Numerical Methods in Engineering, Vol. 3, No. 2, 1971, pp. 275-90.

3. Pawsey, S. F.; and Clough, R. W.: Improved Numerical Integration of Thick Shell Finite Elements. International Journal for Numerical Methods in Engineering, Vol. 3, 1971, pp. 575-586.

4. Wilson, E. L.; Taylor, R. L.; Doherty, W. P.; and Ghaboussi, T.: Incompatible Displacement Models. Numerical and Computer Methods in Structural Mechanics, Edited by S. T. Fenves et al., Academic Press, 1973, pp. 43-57.

5. Taylor, R. L.; Beresford, P. J.; and Wilson, E. L.: A Non-conforming Element for Stress Analysis. International Journal for Numerical Methods in Engineering, Vol 10, 1976, pp. 1211-1220.

6. Irons, B. M.; and Ahmad, S.: Techniques of Finite Elements. John Wiley and Sons, New York, 1980.

7. Allman, D. J.: A Compatible Triangular Element Including Vertex Rotations for Plane Elasticity Analysis. Computers and Structures, Vol. 19, No. 1-2, 1984, pp. 1-8.

8. Cook, R. D.: On the Allman Triangle and a Related Quadrilateral Element. Computers and Structures, Vol. 22, No. 6, 1986, pp. 1065-1067.

9. MacNeal, R. H.; and Harder R. L.: A Refined Four-Noded Membrane Element with Rotational Degrees of Freedom. Computers and Structures, Vol. 28, No. 1, 1988, pp. 75-84.

10. Yunus, S. H.; Saigal S.; and Cook, R. D.: On Improved Hybrid Finite Elements with Rotational Degrees of Freedom. International Journal for Numerical Methods in Engineering, Vol. 28, 1989, pp. 785-800.

11. Aminpour, M. A.: A 4-Node Assumed-Stress Hybrid Shell Element with Rotational Degrees of Freedom. NASA CR-4279, 1990.

12. Pian, T. H. H.: Evolution of Assumed Stress Hybrid Finite Element. Accuracy, Reliability and Training in FEM Technology, Proceedings of the Fourth World Congress and Exhibition on Finite Element Methods, The Congress Center, Interlaken, Switzerland, Edited by John Robinson, September 17-21, 1984, pp. 602-619.

13. Pian, T. H. H.; and Sumihara K.: Rational Approach for Assumed Stress Finite Elements. International Journal for Numerical Methods in Engineering, Vol. 20, 1984, pp. 1685-1695.

14. Pian, T. H. H.: Finite Elements Based on Consistently Assumed Stresses and Displacement. Finite Elements in Analysis and Design, Vol. 1, 1985, pp. 131-140.

15. Pian, T. H. H.; and Chen, D.: On the Suppression of Zero Energy Deformation Modes. International Journal for Numerical Methods in Engineering, Vol. 19, 1983, pp. 1741-1752.

16. Friedrichs, K. O.; and Dressler, R. F.: A Boundary-Layer Theory for Elastic Plates. Communications on Pure and Applied Mathematics, Vol. 14, 1961, pp. 1-33.

17. Reiss, E. L.; and Locke, S.: On the Theory of Plane Stress. Quarterly of Applied Mathematics, Vol. 19, No. 3, 1961, pp. 195-203.

18. Laws, N.: A Boundary-Layer Theory for Plates with Initial Stress. Cambridge Philosophical Society Proceedings, Vol. 62, 1966, pp. 313-327.

19. Kang, D.: Hybrid Stress Finite Element Method. Ph.D. Dissertation, Massachusetts Institute of Technology, Cambridge, MA, May 1986.

20. Reissner, E.: On Bending of Elastic Plates. Quarterly of Applied Mathematics, Vol. 5, 1947, pp. 55-68.

21. Knight, N. F., Jr.; Gillian, R. E.; McCleary, S. L.; Lotts, C. G.; Poole, E. L.; Overman, A. L.; and Macy, S. C.: CSM Testbed Development and Large-Scale Structural Applications. NASA TM-4072, April 1989.

22. Stanley, G. M.; and Nour-Omid, S.: The Computational Structural Mechanics Testbed Generic Structural-Element Processor Manual. NASA CR-181728, March 1990.

23. MacNeal, R. H.; and Harder, R. L.: A Proposed Standard Set of Problems to Test Finite Element Accuracy. Finite Elements in Analysis and Design, Vol. 1, No. 1, 1985, pp. 3-20.

24. Timoshenko, S. P.; and Goodier, J. N.: Theory of Elasticity. McGraw-Hill, Third Edition, 1970.

25. Scordelis, A. C.; and Lo, K. S.: Computer Analysis of Cylindrical Shells. Journal of the American Concrete Institute, Vol. 61, 1969, pp. 539-561.

26. MacNeal, R. H.: A Simple Quadrilateral Shell Element. Computers and Structures, Vol. 8, 1978, pp. 175-183.

27. Park, K. C.; and Stanley, G. M.: A Curved C^0 Shell Element Based on Assumed Natural-Coordinate Strains. Journal of Applied Mechanics, Vol. 108, 1986, pp. 278-290.

28. Stanley, G. M.: Continuum-Based Shell Elements. Ph.D. Dissertation, Stanford University, Stanford, CA, August 1985.

29. Rankin, C. C.; Stehlin, P.; and Brogan, F. A.: Enhancements to the STAGS Computer Code. NASA CR-4000, 1986.

30. Aminpour, M. A.: Assessment of SPAR Elements and Formulation of Some Basic 2-D and 3-D Elements for Use with Testbed Generic Element Processor. Proceedings of NASA Workshop on Computational Structural Mechanics - 1987, NASA CP-10012-Part 2, Nancy P. Sykes, (Editor), 1989, pp. 653-682.

Appendix

The following is a brief description of the elements (except the present element) used in Tables 1-5 for comparison with the present element.

The QUAD4 MSC/NASTRAN element is a 4-node isoparametric shell element with selective reduced-order integration. The transverse shear uses a string-net approximation and augmented shear flexibility[26]. This element was developed by MacNeal and is available in the MSC/NASTRAN finite element code.

The Q4S element is a 4-node shell element in which the membrane part is formulated internally as an 8-node isoparametric element with selective reduced-order integration and later reduced to a 4-node element by eliminating the midside degrees of freedom in favor of rotational degrees of freedom at the corner nodes. This element was developed by MacNeal[9]. The bending part of the Q4S is the same as that of the QUAD4[9].

The AQ element is a 4-node assumed-stress hybrid/mixed membrane element which is formulated internally as an 8-node isoparametric membrane element and later reduced to a 4-node membrane element by eliminating the midside degrees of freedom in favor of rotational degrees of freedom at the corner nodes. This element was formulated by Yunus et al.[10]. The only result reported in reference [10] for the cantilever beam problem in Table 1 using the AQ element is for the mesh with trapezoidal-shaped elements with a unit in-plane end moment. This result is reported to be .85. The difference in the results between the AQ membrane element and membrane part of the the AQR8 element described earlier is in the selection of the assumed-stress functions.

The ES1/EX47 element is a 4-node C^0 isoparametric assumed natural-coordinate strain (ANS) shell element developed by Park and Stanley (see, references [27-28]) and implemented in the CSM Testbed Software System[21] by Stanley using the generic element processor template[22]. This element is not invariant and does not pass the patch test. This element does not include the drilling degrees of freedom in the formulation.

The ES5/E410 element is a 4-node C^1 shell element which was originally implemented in the STAGS finite element code and later in the CSM Testbed by Rankin[29]. This element includes the rotational degrees of freedom in the formulation and uses cubic interpolation for all the displacement fields. This element is not invariant and does not pass the patch test.

The ES4/EX43 element is a simple 4-node C^0 isoparametric assumed-stress hybrid/mixed shell element implemented in the CSM Testbed by this author[30]. This element passes the patch test and is invariant with respect to node numbering. This element does not include the drilling degrees of freedom in the formulation and uses linear interpolation for all displacement and rotation fields.

The AQR8 element is a 4-node shell element which is formulated internally as an 8-node isoparametric assumed-stress hybrid/mixed element and later reduced to a 4-node element by eliminating the midside degrees of freedom in favor of rotational degrees of freedom at the corner nodes[11]. This element was also developed and implemented in the CSM Testbed by this author.

Table 1. Normalized tip displacements in direction of loads for straight cantilever beam.

Tip Loading / Direction	QUAD4 MSC/ NASTRAN	ES1/ EX47†	ES5/ E410†	ES4/ EX43	AQR8‡	AQD4 (present)
(a) rectangular shape elements						
Extension	.995	.995	.994	.996	.998	.998
In-plane Shear	.904*	.904	.915	.993	.993	.993
Out-of-Plane Shear	.986	.980	.986	.981	.981	.981
Twist	.941**	.856	.680	1.023	1.011	1.011
End Moment	—	.910	.914	1.000	1.000	1.000
(b) trapezoidal shape elements						
Extension	.996	.761	.991	.999	.998	.998
In-plane Shear	.071*	.305	.813	.052	.986	.986
Out-of-Plane Shear	.968	.763	#	.075	.965	.965
Twist	.951**	.843	#	1.034	1.029	1.009
End Moment	—	.505	.822	.102	.996	.995
(c) parallelogram shape elements						
Extension	.996	.966	.989	.999	.998	.998
In-plane Shear	.080*	.324	.794	.632	.977	.972
Out-of-Plane Shear	.977	.939	.991	.634	.980	.980
Twist	.945**	.798	.677	1.166	1.159	1.010
End Moment	—	.315	.806	.781	.989	.986

† These elements are not invariant and do not pass the patch test.

‡ Assumed-stresses are in the natural coordinates and do not, in general, satisfy the equilibrium equations (see Ref. [11]).

* The results from MacNeal's Q4S element for in-plane shear load are reported in reference [9] to be .993, .988, and .986 for the meshes (a), (b), and (c) in Fig. 4 respectively.

** These results for twist were normalized with .03028 in reference [23]. Herein, all the other results for twist are normalized using .03046 according to Timoshenko and Goodier's Theory of Elasticity[24].

\# The element produces a singular stiffness matrix for this mesh.

Table 2. Normalized tip displacements in direction of loads for curved cantilever beam.

Tip Loading Direction	QUAD4 MSC/ NASTRAN	ES1/ EX47	ES5/ E410	ES4/ EX43	AQR8	AQD4 (present)
In-plane Shear	.833	.929	.938	.888	.997	.996
Out-of-Plane Shear	.951	.935	.887	.925	.956	.956

Table 3. Normalized vertical deflection at point C for the tapered and swept panel.

Mesh	AQ	ES1/ EX47	ES5/ E410	ES4/ EX43	AQR8	AQD4 (present)
2×2	.914	.880	.873	.882	.930	.926
4×4	.973	.953	.953	.962	.979	.979

Table 4. Normalized displacements at the midpoint of the free-edge for Scordelis-Lo roof.

Mesh	QUAD4 MSC/ NASTRAN	ES1/ EX47	ES5/ E410	ES4/ EX43	AQR8	AQD4 (present)
2×2	1.376	1.387	1.384	1.459	1.218	1.218
4×4	1.050	1.039	1.049	1.068	1.021	1.021
6×6	1.018	1.011	1.015	1.028	1.006	1.006
8×8	1.008	1.005	1.005	1.017	1.003	1.003
10×10	1.004	1.003	1.001	1.011	1.001	1.001

Table 5. Normalized displacements at load points for hemispherical shell problem.

Mesh	QUAD4 MSC/ NASTRAN	ES1/ EX47	ES5/ E410	ES4/ EX43	AQR8	AQD4 (present)
2×2	.972	.968	.338	1.032	.382	.381
4×4	1.024	1.018	.519	1.093	.227	.226
6×6	1.013	1.001	.841	1.060	.432	.432
8×8	1.005	.995	.949	1.040	.681	.680
10×10	1.001	.993	.978	1.027	.835	.835
12×12	.998	.992	.988	1.020	.914	.914

† The drilling degrees of freedom for these elements were not suppressed in this problem.

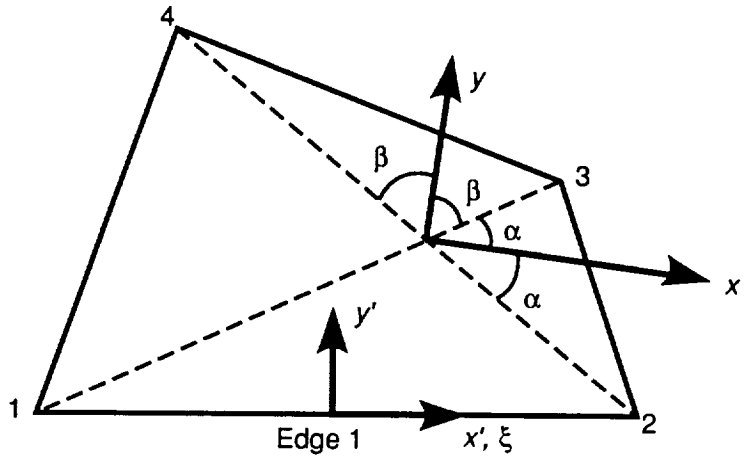

Figure 1. Element coordinate system definition.

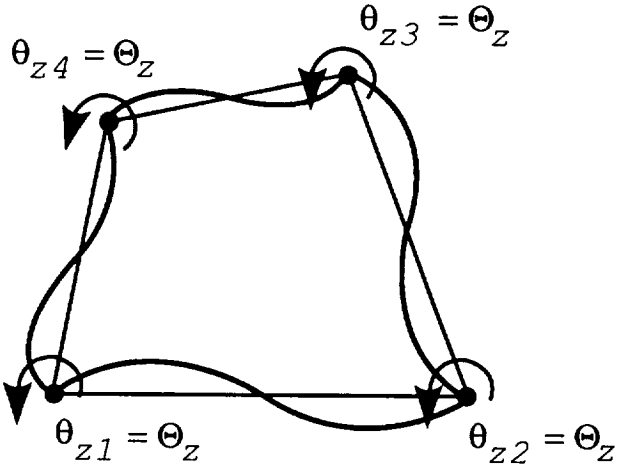

Figure 2. The "zero displacement" mode.

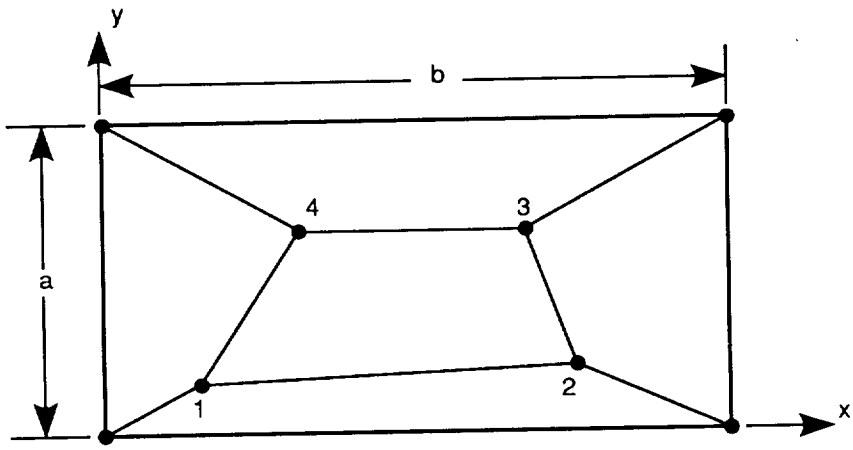

Location of nodes:

node	x	y
1	.04	.02
2	.18	.03
3	.16	.08
4	.08	.08

Applied displacements:

(a) Membrane patch test

Boundary conditions: $u = 10^{-3}(x + y/2)$
$v = 10^{-3}(x/2 + y)$

Theoretical solution: $\epsilon_{xx} = \epsilon_{yy} = \gamma_{xy} = 10^{-3}$
$\sigma_{xx} = \sigma_{yy} = 1333.$, $\sigma_{xy} = 400.$

(b) Bending patch test

Boundary conditions: $w = -10^{-3}(x^2 + xy + y^2)/2$
$\theta_x = -10^{-3}(x/2 + y)$
$\theta_y = -10^{-3}(x + y/2)$

Theoretical solution:

Bending moments per unit length:

$M_x = M_y = 1.111\times10^{-7}$, $M_{xy} = 3.333\times10^{-8}$

Surface stresses:

$\sigma_{xx} = \sigma_{yy} = \pm0.667$, $\sigma_{xy} = \pm0.200$

Figure 3. The patch test problem. a=0.24, b=0.12, t=0.001, E=10^6, ν=0.25. (Consistent units are used for various properties.)

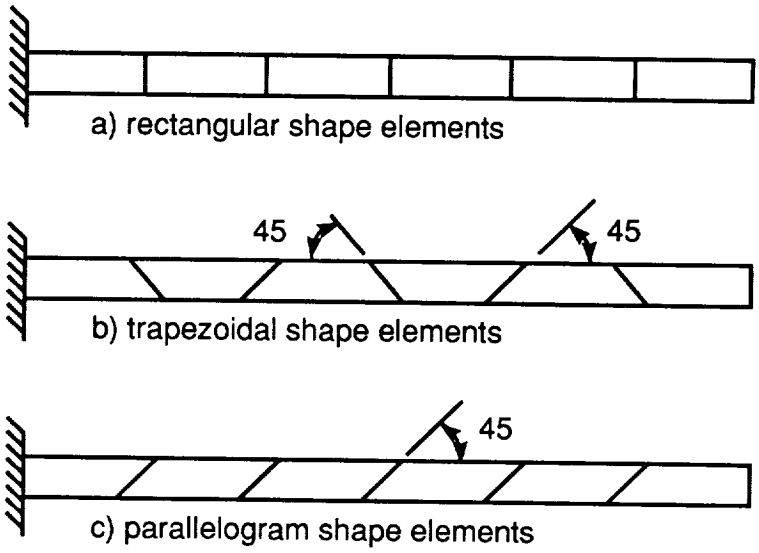

Theoretical solutions:

Tip load direction	Displacement in direction of load
Extension	$.3\times10^{-4}$
In-plane shear	.1081
Out-of-plane shear	.4321
Twist	.03406
In-plane moment	.009

Figure 4. Straight cantilever beam problem. Length=6., height=0.2, depth=0.1, E=10^7, ν=0.3, mesh=6×1. Loading: unit forces at the free end.

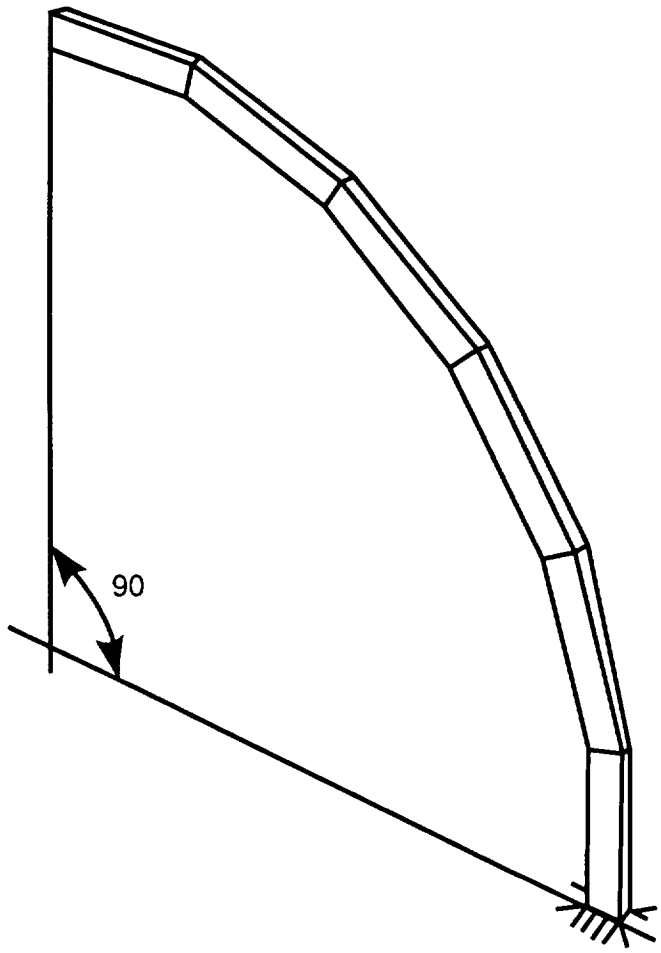

Theoretical solutions:

Tip load direction	Displacement in direction of load
In-plane shear	.08734
Out-of-plane shear	.5022

Figure 5. The curved cantilever beam problem. Inner radius=4.12, outer radius=4.32, depth=0.1, E=10^7, ν=0.25, mesh=6×1. Loading: unit forces at the free end. (Consistent units are used for various properties.)

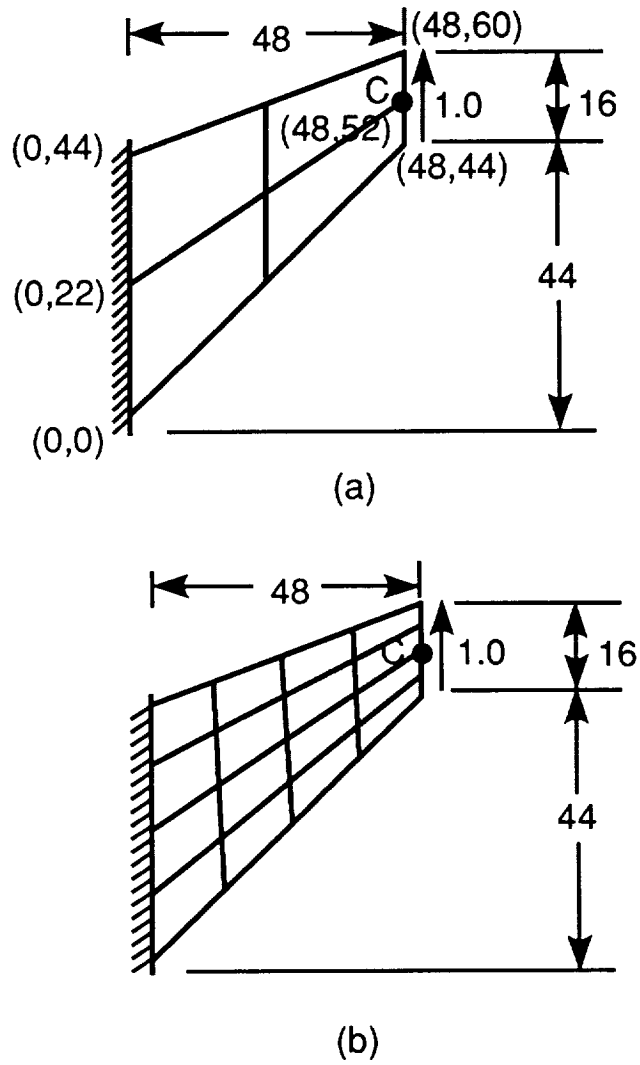

Figure 6. The tapered and swept panel problem. Thickness=1., E=1., ν=1/3, mesh=N×N. Loading: unit in-plane shear force distributed on the free edge. Reference solution: vertical displacement at C=23.90 from reference [10]. (a) 2×2 mesh, (b) 4×4 mesh.
(Consistent units are used for various properties.)

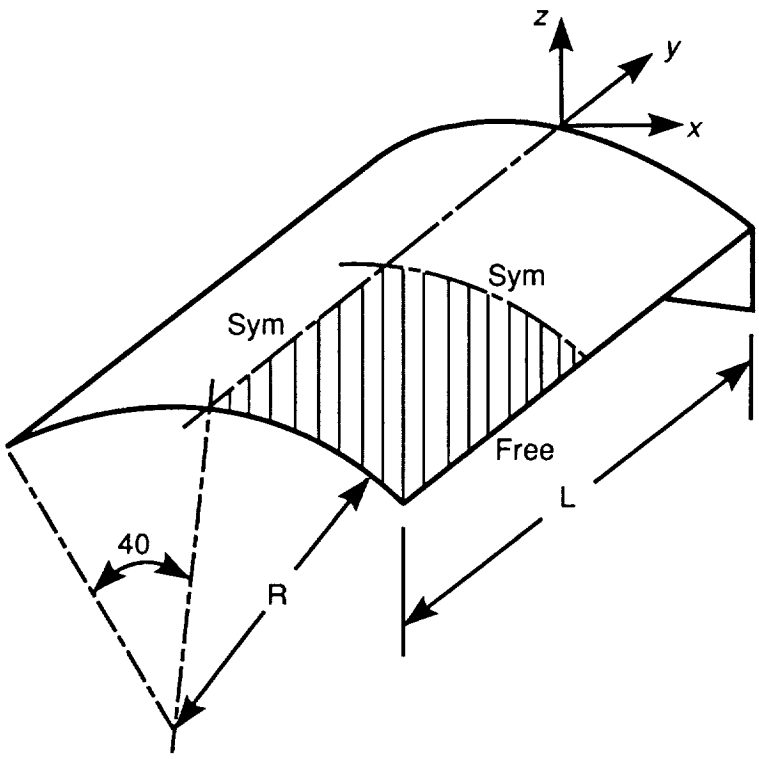

Figure 7. The Scordelis-Lo roof problem. Length=50., radius=25., thickness=0.25, E=4.32×10^8, ν=0.3, mesh=N×N. Loading: 90. per unit area in vertical direction, *i.e.*, gravity load; u_x=u_z=0 on curved edges. Reference solution: vertical displacement at midpoint of free-edge=0.3024 from reference [23].
(Consistent units are used for various properties.)

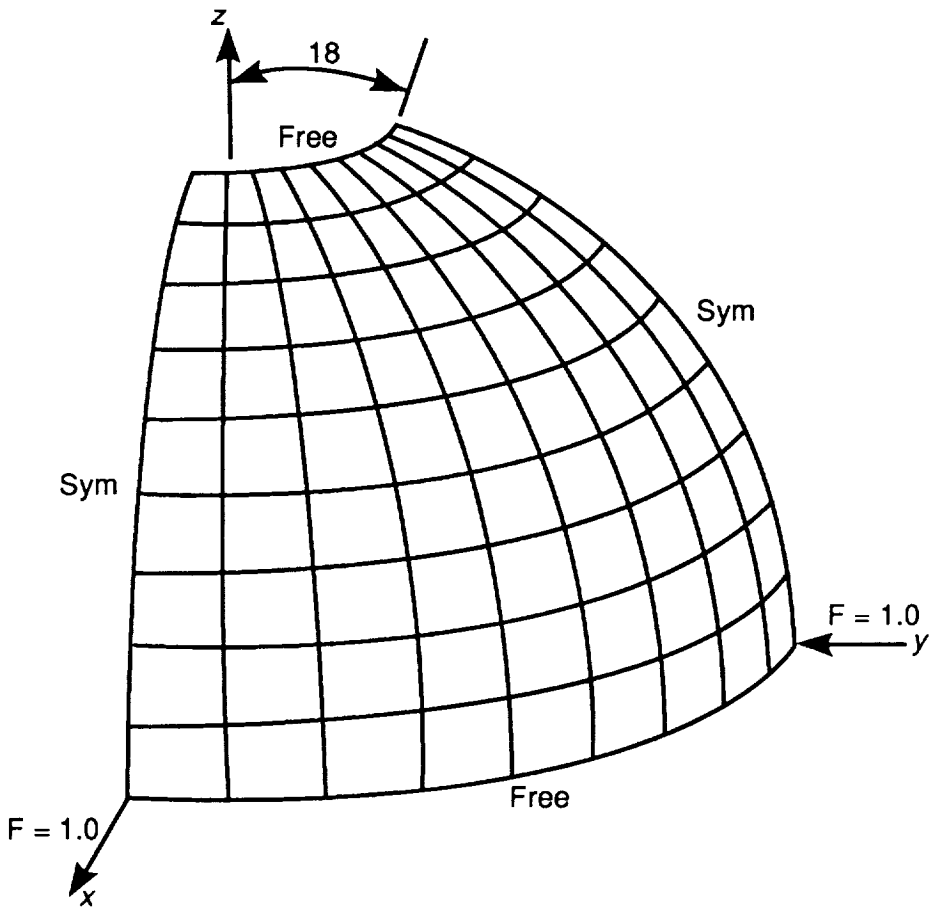

Figure 8. The spherical shell problem. Radius=10., thickness=0.04, E=6.825×10^7, ν=0.3, mesh=N×N. Loading: concentrated forces as shown. Reference solution: radial displacement at the load points=0.0940 from reference [23]. (Consistent units are used for various properties.)

NASA
National Aeronautics and Space Administration

Report Documentation Page

1. Report No.	2. Government Accession No.	3. Recipient's Catalog No.
NASA CR-4282		

4. Title and Subtitle	5. Report Date
Direct Formulation of a 4-Node Hybrid Shell Element With Rotational Degrees of Freedom	April 1990
	6. Performing Organization Code
7. Author(s)	8. Performing Organization Report No.
Mohammad A. Aminpour	
9. Performing Organization Name and Address	10. Work Unit No.
Analytical Services and Materials, Inc. Hampton, VA 23666	505-63-01-10
	11. Contract or Grant No.
	NAS1-18599
12. Sponsoring Agency Name and Address	13. Type of Report and Period Covered
National Aeronautics and Space Administration Langley Research Center Hampton, VA 23665-5225	Contractor Report
	14. Sponsoring Agency Code

15. Supplementary Notes

Langley Technical Monitor: W. Jefferson Stroud

16. Abstract

A simple 4-node assumed-stress hybrid quadrilateral shell element with rotational or "drilling" degrees of freedom is formulated. The element formulation is based directly on a 4-node element. This direct formulation requires fewer computations than a similar element that is derived from an "internal" 8-node isoparametric element in which the midside degrees of freedom are eliminated in favor of rotational degrees of freedom at the corner nodes. The formulation is based on the principle of minimum complementary energy. The membrane part of the element has 12 degrees of freedom including rotational degrees of freedom. The bending part of the element also has 12 degrees of freedom. The bending part of the element uses the Reissner-Mindlin plate theory which takes into account the transverse shear effects. Quadratic variations for both in-plane and out-of-plane displacement fields and linear variations for both in-plane and out-of-plane rotation fields are assumed along the edges of the element. The element Cartesian-coordinate system is chosen such as to make the stress field invariant with respect to node numbering. The membrane part of the stress field is based on a 9-parameter equilibrating stress field, while the bending part is based on a 13-parameter equilibrating stress field. The element passes the patch test, is nearly insensitive to mesh distortion, does not "lock," possesses the desirable invariance properties, has no spurious modes, and produces accurate and reliable results.

17. Key Words (Suggested by Authors(s))	18. Distribution Statement
assumed-stress, hybrid, quadrilateral, shell, rotational, drilling, element, finite element, variational	Unclassified—Unlimited Subject Category 39

19. Security Classif.(of this report)	20. Security Classif.(of this page)	21. No. of Pages	22. Price
Unclassified	Unclassified	28	A03

NASA FORM 1626 OCT 86

For sale by the National Technical Information Service, Springfield, Virginia 22161-2171

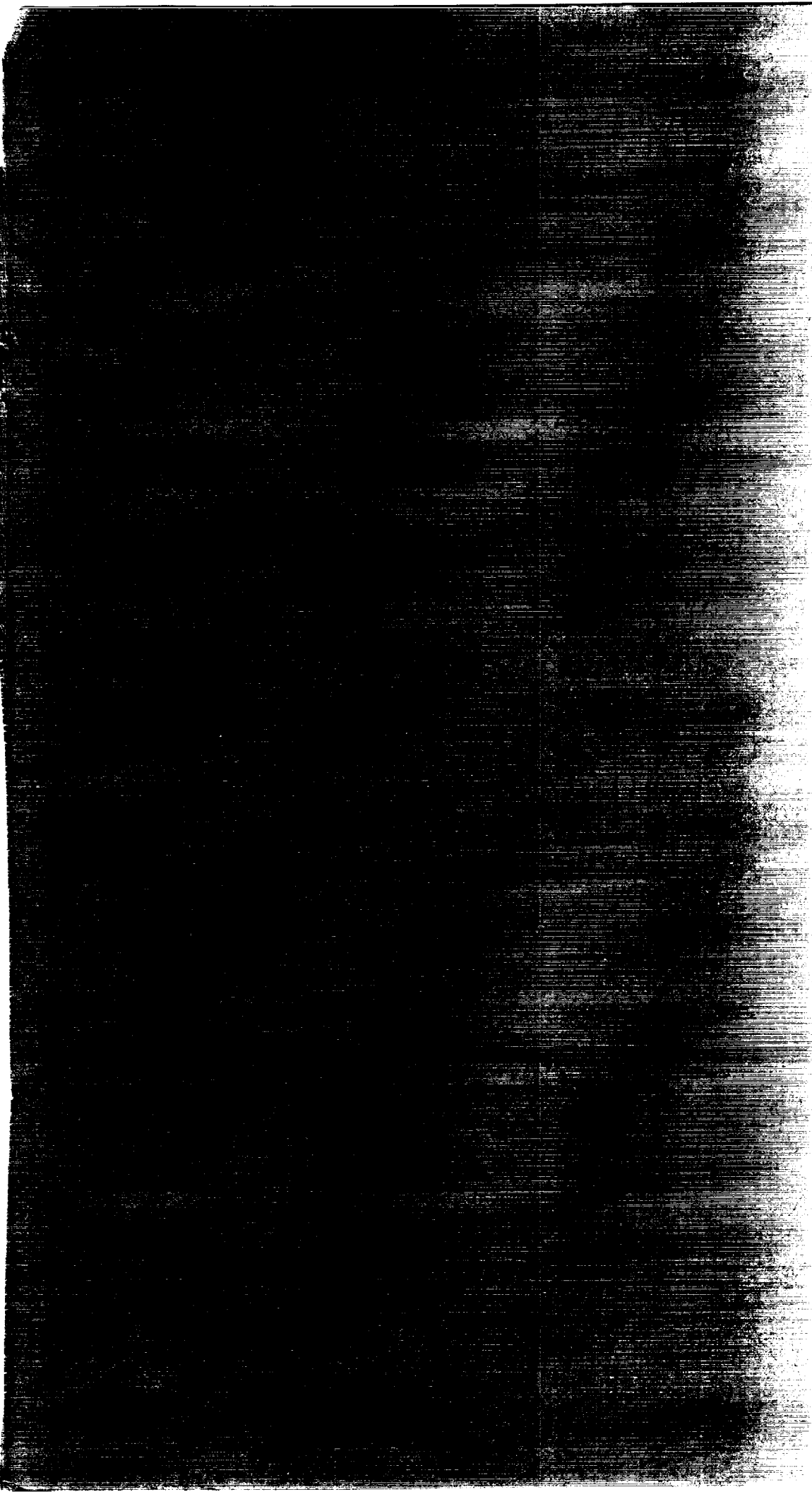

...l Aeronautics and
... Administration
...-4
Washington, D.C.
...0001

NASA